American Journal of Cancer Biomedical Imaging
American Journal of Biomedical Imaging
http://www.ivyunion.org/index.php/ajbi/index
Vo1. 1, Article ID 20130133, 12 pages

Research Article

Automatic Detection of Vasculature from the Images of Human Retina Using CLAHE and Bitplane Decomposition

Ashok kumar T[1*], Priya S[2], Varghese Paul[3]
[1]College of Engineering, Cherthala, Kerala, India
[2]Govt.Model Engineering College, Thrikkakara,Kerala, India
[3]Cochin University of Science and Technology, Cochin,Kerala, India
ashokkumart@yahoo.com

Abstract

Retinal blood vessel detection and extraction is an essential step in understanding several eye related pathologies. It is the key in automatic screening systems for retinal abnormalities. We present a novel yet simple approach to the detection and segmentation of vasculature from the fundus images of the human retina. For the detection and extraction of blood vessels, the green channel of the image is separated. The green channel is preprocessed for a better contrast by using contrast limited adaptive histogram equalization (CLAHE) and mathematical morphology. On applying bitplane decomposition, bitplane 2 is found to carry important information on the topology of retinal vasculature. A series of morphological operations on bitplane 2 segment the vasculature accurately. The proposed algorithm is computationally simple and does not require a prior knowledge of other retinal features like optic disc and macula. The algorithm has been evaluated on a subset of MESSIDOR and DRIVE image databases with various visual qualities. Robustness with respect to changes in the parameters of the algorithm has been examined.

Keywords: adaptive histogram equalization; bitplane decomposition; bottom hat transform; fundus images mathematical morphology; top hat transform
Peer Reviewer: Sihua Peng, PhD，Department of Pathology，Zhejiang University School of Medicine, China
Received: April 21, 2013; **Accepted**: July 3, 2013; **Published:** August 18, 2013
Competing Interests: The authors have declared that no competing interests exist.

***Correspondence to:** Ashok Kumar T. College of Engineering, Cherthala, Kerala, India
Email: ashokkumart@yahoo.com

Introduction

For the diagnosis of eye related pathologies, digital fundus images are becoming increasingly popular. This fact opens up the possibility of applying digital image processing techniques in ocular fundus images to facilitate and improve diagnosis in different ways [1]. Several studies were carried out on the segmentation of blood vessels in general, however only a small number of them were associated with retinal blood vessels. Reliable and robust vessel extraction is a pre requisite for subsequent retinal image analysis and processing since vessels are the predominant and most stable structures appearing in these images. Computer-aided detection and analysis

of retinal images play a pivotal role in modern diagnostic procedures. However, automatic retinal segmentation is a complicated affair because of the fact that retinal images are often noisy, poorly contrasted, and there is a wide variation in vessel widths. Information on the retinal vasculature can be used in grading disease severity or as part of the process of automated diagnosis of ophthalmic pathologies. Appearance of the blood vessels in the retina can provide information on pathological changes caused by some diseases including diabetes, hypertension, arteriosclerosis and retinopathy of prematurity. The effectiveness of treatment for many eye related diseases lies in early detection through regular screenings. Furthermore, segmentation of the vascular tree in the retina seems to be the most appropriate representation for image registration applications due to the following three reasons:

(i) it maps the whole retina;
(ii) it does not move except in case of a few diseases;
(iii) it contains enough information for the localization of some anchor points [2].

Many published algorithms for optic disc detection, image registration, change detection, pathology detection and quantification, tracking in video sequences, and computer-aided screening systems depend on vessel extraction [3]. The techniques published in the research literature for retinal blood vessel extraction can be broadly classified into methods based on matched filters, adaptive thresholds, intensity edges, region growing, statistical inferences, mathematical morphology and Hessian measures. The recent literature has been dominated by Hessian-based methods because of their utility in characterizing the elongated structure of vessels. Several challenges of vessel extraction in retinal images are illustrated in literature. These are:

(i) There is a wide range of vessel widths.
(ii) Vessels may be of low contrast. The central intensity of some vessels differs from the background. Narrow vessels generally exhibit the lowest contrast.
(iii) A variety of structures appear in retinal images, including the retina boundary, the optic disc, and various pathologies. The latter are a particular challenge for automatic vessel extraction since they appear as a series of bright spots, sometimes with narrow, darker gaps in between.
(iv) Wider vessels sometimes have a bright strip running down the center (the “central reflex”), causing a rather complicated intensity cross-section. Locally, this may be hard to distinguish from two side-by-side vessels.

Our primary focus in this paper is to extract the vasculature accurately along with narrow vessels, while avoiding false responses.

Background

There are many methods in published literature for the detection of blood vessel tree in retinal images. The method presented by Chaudhari *et al*. [4] is primarily based on 2-D matched filter. The concept of matched filter algorithm is employed for the detection of piecewise linear segment of retinal blood vessels. Hoover *et al*. [5] improved the methodology in [4] by threshold probing. The result obviously shows an increase in true positive rate over basic thresholding of a matched filter. Kande *et al*. [6] also uses matched filter in [4] to detect vessel tree. The improvised result is achieved by using thresholding algorithm based on the Spatially Weighted Fuzzy C-Means (SWFCM) clustering. Staal *et al*. [7] proposed an automated segmentation of vessels in two-dimensional color images of the retina. This method is based on extraction of image ridges and approximates the vessel centerlines at the same time. Akram *et al*. [8] and Oloumi *et al*. [9] detected the vascular pattern and thin vessels by using 2-D Gabor wavelet. Sofka and Stewart [3] made an improvement in blood vessel detection in the context of low-contrast and tried to detect the narrow vessels by multi-scale matched

filters. The algorithm combines matched-filter responses, confidence measures and vessel boundary measures. After combining these responses, it forms a six-dimensional measurement vector at each pixel. Then a training technique is used to map this vector to likelihood ratio vesselness which is used for the vesselness measurement at each pixel. A supervised approach based on artificial neural network (ANN) was proposed for blood vessel extraction in [10] and [11]. The sensitivity and specificity achieved by the method are quite high, however post-processing was required to do away with the misclassified vessels.

The methods mentioned above work well to detect the main parts of the vessel tree. However, it does not perform well to extract the narrow vessels. Since the vessels have a wide range of width and the area of small width usually has very low contrast, it simply misses to identify it as a vessel. In addition, detection of non-vascular structure such as camera aperture boundary and the optic disc along with the vascular structure is of concern. In an attempt to address the above problem, a vessel extraction algorithm based on contrast limited adaptive histogram equalization and mathematical morphology is proposed in this paper.

Methodology

Adaptive Histogram Equalization

Adaptive histogram equalization (AHE) is an image processing technique used to improve contrast in images. It differs from ordinary histogram equalization in the respect that the adaptive method computes several histograms, each corresponding to a distinct section of the image, and uses them to redistribute the lightness values of the image. It is therefore suitable for improving the local contrast of an image and bringing out more detail.

However, AHE has a tendency to over amplify noise in relatively homogeneous regions of an image. A variant of adaptive histogram equalization called contrast limited adaptive histogram equalization (CLAHE) prevents this by limiting the amplification [12]. Ordinary histogram equalization uses the same transformation derived from the image histogram to transform all pixels. This works well when the distribution of pixel values is similar throughout the image. However, when the image contains regions that are significantly lighter or darker than most of the image, the contrast in those regions will not be sufficiently enhanced.

In its simplest form, each pixel is transformed based on the histogram of a square surrounding the pixel. The derivation of the transformation functions from the histograms is exactly the same as for ordinary histogram equalization. The transformation function is proportional to the cumulative distribution function (CDF) of pixel values in the neighborhood.

Pixels near the image boundary have to be treated specially, because their neighborhood would not lie completely within the image. This can be solved by extending the image by mirroring pixel lines and columns with respect to the image boundary. Simply copying the pixel lines on the border is not appropriate, as it would lead to a highly peaked neighborhood histogram.

CLAHE differs from ordinary adaptive histogram equalization in its contrast limiting. This feature can also be applied to global histogram equalization, giving rise to contrast-limited histogram equalization (CLAHE), which is rarely used in practice. In the case of CLAHE, the contrast limiting procedure has to be applied for each neighborhood from which a transformation function is derived. CLAHE was developed to prevent the over amplification of noise that adaptive histogram equalization can give rise to. This is achieved by limiting the contrast enhancement of AHE. The contrast amplification in the vicinity of a given pixel value is given by the slope of the transformation function. This is proportional to the slope of the neighborhood cumulative distribution function (CDF) and therefore to the value of the histogram at that pixel value. CLAHE limits the amplification by clipping the histogram at a predefined

value before computing the CDF. This limits the slope of the CDF and therefore of the transformation function. The value at which the histogram is clipped, the so-called clip limit, depends on the normalization of the histogram and thereby on the size of the neighborhood region. Common values limit the resulting amplification to between 3 and 4.

It is advantageous not to discard the part of the histogram that exceeds the clip limit but to redistribute it equally among all histogram bins. The redistribution will push some bins over the clip limit again, resulting in an effective clip limit that is larger than the prescribed limit and the exact value of which depends on the image. If this is undesirable, the redistribution procedure can be repeated recursively until the excess is negligible.

Adaptive histogram equalization in its straightforward form presented above, both with and without contrast limiting, requires the computation of a different neighborhood histogram and transformation function for each pixel in the image. This makes the method very expensive computationally.

Interpolation allows a significant improvement in efficiency without compromising the quality of the result. The image is partitioned into equally sized rectangular tiles .A common choice is 64 tiles in 8 columns and 8 rows. A histogram, CDF and transformation function is then computed for each of the tiles. The transformation functions are appropriate for the tile center pixels. All other pixels are transformed with up to four transformation functions of the tiles with center pixels closest to them, and are assigned interpolated values. Pixels in the bulk of the image are bilinearly interpolated, pixels close to the boundary are linearly interpolated, and pixels near corners are transformed with the transformation function of the corner tile. The interpolation coefficients reflect the location of pixels between the closest tile center pixels, so that the result is continuous as the pixel approaches a tile center. This procedure reduces the number of transformation functions to be computed dramatically and only imposes the small additional cost of linear interpolation.

Biplane Decomposition

The grey level of each pixel in a digital image is stored as one or more bytes in the computer. When the grey level is represented as a single byte, it is called an 8 bit image, representing grey level values in the range 0 to 255. Decomposing a digital image into its bit planes is useful for analyzing the relative importance played by each bit of the image. Instead of highlighting gray level images, highlighting the contribution made to total image appearance by specific bits is examined here. In a representative 8 bit gray level image, each pixel in an image is represented by 8 bits. The image is composed of 8, 1-bit planes ranging from bit plane 0 (LSB) to bit plane 7 (MSB). In terms of 8-bits, plane 0 contains all the lowest order bits in the bytes comprising the pixels in the image and plane 7 contains all the higher order bits. Thus bitplane decomposition of an 8 bit image yields eight binary images. The bit-plane representation of an 8 bit image is shown in Fig. 1

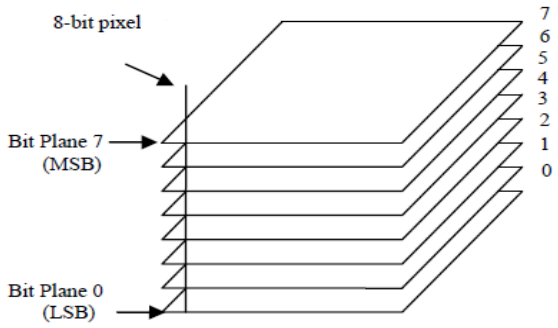

Figure 1 Bitplane decomposition

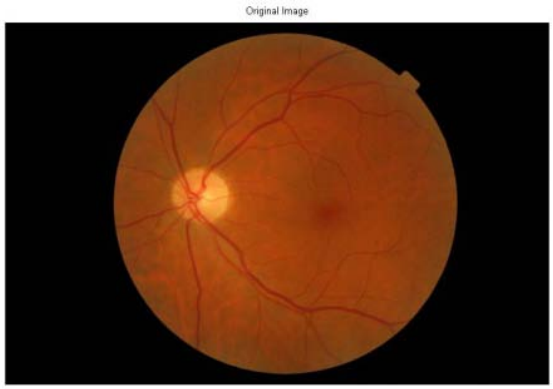

Figure 2 Original Image

In general, the higher order bit planes contain a majority of visually significant data while the lower order ones contribute to more subtle details in an image. On examining the eight bit planes of the image, the bitplane 2 is found to carry vital information on the vessel tree in the retinal image.

For the pre-processed retinal images, bit-plane 2 is carrying significant information corresponding to the vascular tree. Bit-plane 2 of the chosen image is shown in Fig. 7. As bit-plane images are binary images, they are highly suited for subsequent morphological image processing.

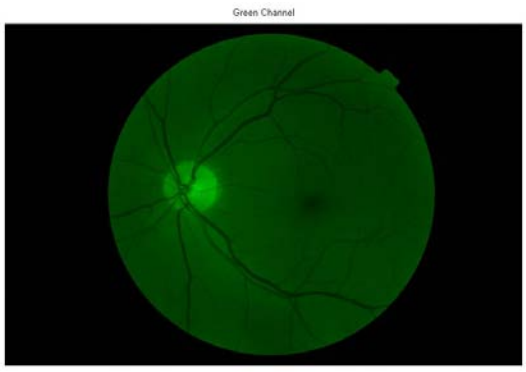

Figure 3 Green Channel of the Original Image

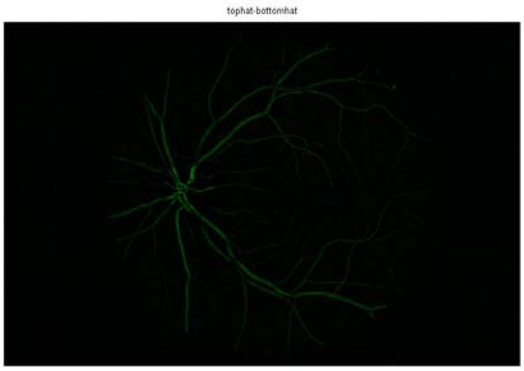

Figure 4 Contrast Enhanced Image

Figure 5 Resultant of CLAHE of Green Channel

] employ ing the techniques of mathematical morphology, the retinal vasculature can be extracted very accurately from the image as shown in Fig 8.

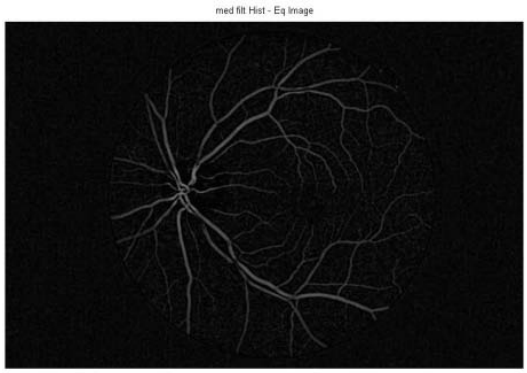

Figure 6 Images after median filtering

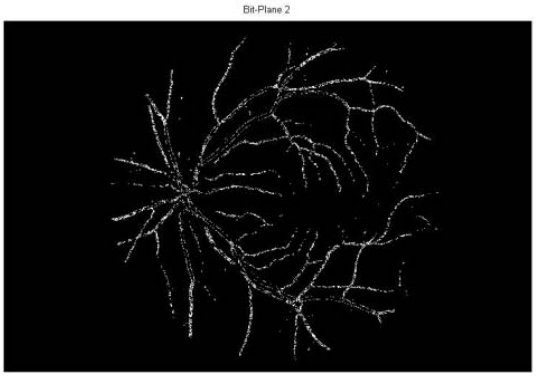

Figure 7 Bit-plane 2

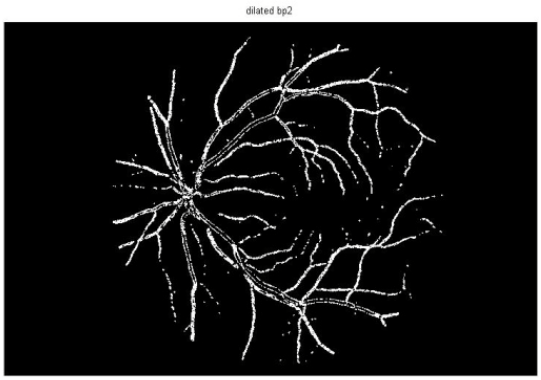

Figure 8 Extracted Blood Vessels from Bit-plane 2

Mathematical Morphology

Mathematical morphology (MM) is the science of appearance, shape and organization. MM deals with non-linear processes which can be applied to an image to remove details smaller than a certain reference shape called the structuring element [13]. MM is also the foundation of morphological image processing, which consists of a set of operators that transform images according to the above characterizations. The most widely used morphological operations used in image processing are dilation, erosion, opening and closing.

MM was originally developed for binary images, and was later extended to grayscale functions and images. In MM, top-hat transform is an operation that extracts small elements and details from given images. There exist two types of top-hat transforms. The white top-hat transform, which is defined as the difference between the input image and its opening by some structuring element, and the black top-hat transform (bottom hat transform) which is defined as the difference between the closing and the input image. Top-hat transforms are used for various image processing tasks, such as feature extraction, background equalization, image enhancement, and others. Binary images are best suited for performing morphological operations. The images obtained after bit plane decomposition are binary images, which are thus suitable for performing morphological operations [14].

Dilation is an operation in which the binary image is expanded from its original shape. The degree of expansion is controlled by the structuring element. The dilation process is similar to convolution, in which the structuring element is reflected and shifted from left to right and then from top to bottom. In this process, any overlapping pixels under the centre position of the structuring element are assigned with 1 or black values. If X is the reference image and B is the structuring element, the dilation of X by B is represented as

$$X \oplus B = \left\{ Z \left| \left[\left(\hat{B} \right)_Z \cap X \right] \subseteq X \right. \right\} \quad (1)$$

Where $\hat{B}$ is the image B rotated about the origin. When an image X is dilated by a structuring element B, the outcome element Z would be that there will be at least one element in B that intersects with an element in X.

Erosion operator is a thinning operator that shrinks an image. The amount by which the shrinking takes place is again determined by the structuring element. Here, if there is a complete overlapping with the structuring

element, the pixel is set white or 0. The erosion of X by B is given as

$$X\Theta B = \left\{ Z\left[\left[\left(\hat{B} \right)_z \right] \subseteq X \right] \right\} \quad (2)$$

In erosion, the outcome element Z is considered only when the structuring element is a subset or equal to the binary image X.

Opening is done by first performing erosion, followed by dilation. Opening smoothens the inside of object contours, breaks narrow strips and eliminates thin portions of the image. It is mathematically represented as

$$X \circ B = (X\Theta B) \oplus B \quad (3)$$

Closing operation does the opposite of opening. It is dilation followed by erosion. Closing fills small gaps and holes in a single pixel object. The closing process is represented by

$$X \bullet B = (X \oplus B)\Theta B \quad (4)$$

Closing operation protects coarse structures, closes small gaps and rounds off concave corners.

Morphological operations are widely used in the detection of boundaries in a binary image. For an image X, the following can be applied to obtain a boundary image

$$Y = X - (X\Theta B) \quad (5)$$

$$Y = (X \oplus B) - X \quad (6)$$

$$Y = (X \oplus B) - (X\Theta B) \quad (7)$$

Where, the operator '$\oplus$' denotes dilation, '$\ominus$' denotes erosion and '$-$' indicates set theoretical subtraction.

Most binary morphological operations have natural extensions to gray scale processing. Some, like morphological reconstruction, have applications that are unique to gray scale images, such as peak filtering.

The Proposed Method

One important issue in fundus images is that retina is not a plane surface and therefore light doesn't have a uniform distribution, producing images with non-uniform illumination and consequently with different contrast areas. Vignetting is often an unintended and undesired effect caused by camera settings or lens limitations. The goal of illumination correction is to remove uneven illumination of the image caused by sensor defaults (vignetting), non uniform illumination of the scene, or orientation of the surface. Retinal image preprocessing consists of correction of non-uniform luminosity, color normalization and contrast enhancement. In this work we use a method of luminosity correction that is based on segmentation of background pixels and subsequent computation of luminosity function based only on the background image [15]. The advantage of this approach is that it does not produce any ringing effect.

From the RGB image, all the three component images are separated. The green channel is found to be having a better contrast as shown in Fig. 3. So only the green channel is preserved for further processing. In order to increase the contrast level, we have taken the bottomhat transform of the green channel. As an attempt to enhance the contrast of the vascular tree, we added this image with the tophat transform of it and then subtracted the bottom hat transform from this combination. The resultant image is shown in Fig. 4. Now contrast limited adaptive histogram equalization (CLAHE) is performed on the resultant image to get

an image as shown in Fig. 5. Subsequently, median filtering is performed to remove the noise components. The resultant image after median filtering is as shown in Fig. 6. On performing bitplane decomposition, we observed that bitplane 2 best represents the vascular tree in the fundus image. A simple dilation with a diamond shaped structuring element will yield the extracted vasculature from the fundus image. Also a series of morphological operations are performed on the binary image to present the results as shown in Fig. 8.

The algorithm has been tested and compared with the commonly used methods and the results show that the method proposed here can not only detect blood vessels but also extract most blood vessels accurately.

Results and Discussion

Blood vessel segmentation is a key step in almost all algorithms used to identify fundus features automatically. Furthermore blood vessel detection is important for automatic diagnosis of other ophthalmic pathologies also. Many automatic techniques for vessel identifcation techniques have been proposed in the literature, with various degrees of complexity and accuracy. The motivation that leads to the development of a new method can be summarized in the following points:

(i) Computational speed,
(ii) Robustness,
(iii) Flexibility to accommodate a wide range of contrast in retinal images.

346 million people worldwide have diabetes. More than 80% of diabetes deaths occur in low- and middle-income countries [16]. Diabetic retinopathy (DR) is a major cause of blindness today. Blindness from DR is responsible for about 20 percent of new cases of blindness between the age group of 45 and 74. Laser photocoagulation can slow down the progression to blindness, if DR is detected in its early stages. However this is not an easy task because DR patients do not perceive symptoms until visual loss develops and this happens in the later stage of the disease, when treatment is less effective. In order to ensure that diabetic patients receive treatment on time, yearly fundus eye examination is advised by physicians. The detection a extraction of vasculature from the retinal images is inevitable for the early detection of ophthalmic pathologies. However growing incidents of diabetes increase the number of patients and as a consequence the number of images that need to be reviewed by experts. In addition, the high cost of examinations and the lack of specialists prevent many patients from receiving effective treatment. Due to these reasons, an expert system for the automatic detection of such anomalies has inspired much research in this direction.

There are large influences of human errors and subjectivity on the results of inspection by a human expert also. Presence of other factors such as noise, non-uniform illumination and variety of defect types in retinal imagery make the detection of features and pathologies in fundus images a challenging problem [17].

Table a comparison of blood vessel extraction algorithms

Method	Accuracy*	Area under ROC	Comments
uman observer	0.9473	--	--
Staal *et. al.*	0.9442	0.952	Supervised
Neimeijer *et. al.*	0.9416	0.9294	Supervised
Kande *et. al.*	0.9437	0.9515	Unsupervised
Zana *et al.*	0.9377	0.8984	Unsupervised
Jiang *et al.*	0.9212	0.9114	Unsupervised
Martnez-Prez *et al.*	0.9181	--	Unsupervised
Chaudhuri *et al.*	0.8773	0.7878	Unsupervised
Onkaew D *et al*	0.9388	0.8557	Unsupervised
Proposed Method	0.9392	0.86805	Unsupervised

* Maximum Average Accuracy

Unfortunately most of the algorithms used today for blood vessel detection are computationally intensive, and are less accurate, particularly in the presence of pathologies in the human retina.

Three performance measures are taken to evaluate the performance of the algorithm and compared it with known best algorithms as shown in Table 1. The first performance measure is receiver operator characteristics (ROC). An ROC space is defined by false positive rate (Fpr) and true positive rate (Tpr) as x and y axes respectively, which depicts relative trade-offs between true positive (benefits) and false positive (costs). Since Tpr is equivalent with sensitivity (Sn) and Fpr is equal to (1 - specificity), the ROC curve is sometimes called the sensitivity vs (1 - specificity) plot. The Sn and Sp are obtained as follows: Both measures are evaluated using the four metric values– true positive (Tp), sum of pixel marked as vessel in both result and ground truth image; false positive (Fp), sum of pixel marked as a vessel in result image but not in ground truth image; false negative (Fn), sum of pixel marked as a background in result image but not in ground truth image; true negative (Tn), sum of pixel marked as a background in both result and ground truth image. The sensitivity and the specificity are computed from Eq. 8 and 9 respectively.

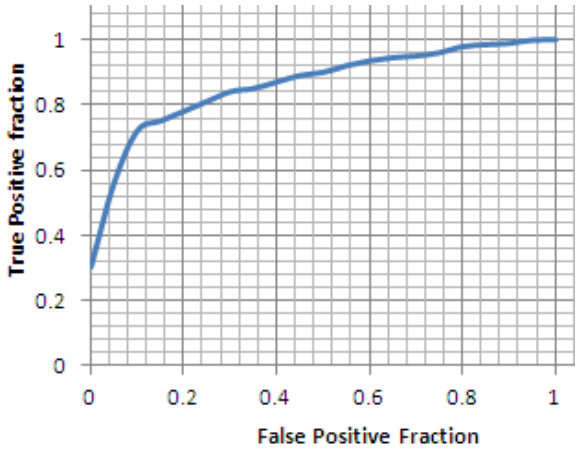

Figure 9 ROC Curve for DRIVE database

The best possible prediction method would yield a point in the upper left corner or coordinate (0,1) of the ROC space, representing 100% sensitivity (no false negatives) and 100% specificity (no false positives) [20]. The (0,1) point is also called a perfect classification. The second is the area under ROC. The larger the area under the curve, the greater the discriminating ability of the segmentation method [21]. The third measure is maximum average accuracy (Maa). The accuracy of an image is calculated by taking the sum of Tn and Tp divided by sum of the total number of nonvessel pixels (n) and total number of vessels (p) as illustrated in Eq. 3. In our experiments, we used the manual segmentation by the first observer of DRIVE database as a gold standard for calculating all these three measures- ROC, area under ROC, and Maa, Only pixels inside the field of view (FOV) are taken into account.

$$Sn = Tpr = \frac{Tp}{(Tp + Fn)} \tag{8}$$

$$Specificity = Tnr = \frac{Tn}{(Tn + Fp)} \tag{9}$$

$$Maa = \frac{(Tn + Tp)}{(p + n)} \tag{10}$$

A comparison of maximum average accuracy of different blood vessel extraction algorithms is as depicted in Fig. 10.

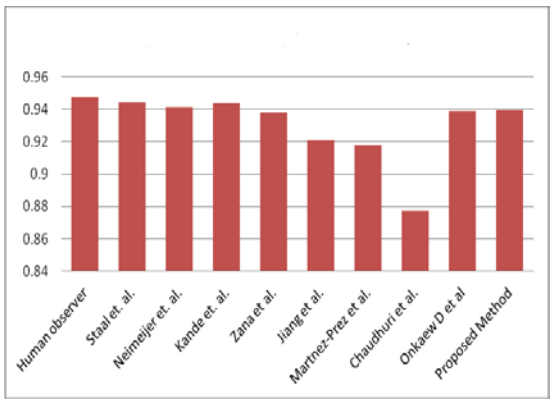

Figure 10 A comparisons based on Maximum average accuracy

A visual comparison of the segmentation results with that of the Ground truth by an expert ophthalmologist (Gold standard) provided in the DRIVE dataset is demonstrated in Fig. 11, Fig. 12 and Fig. 13. An arbitrarily chosen image (Image No 16) is used in this study.

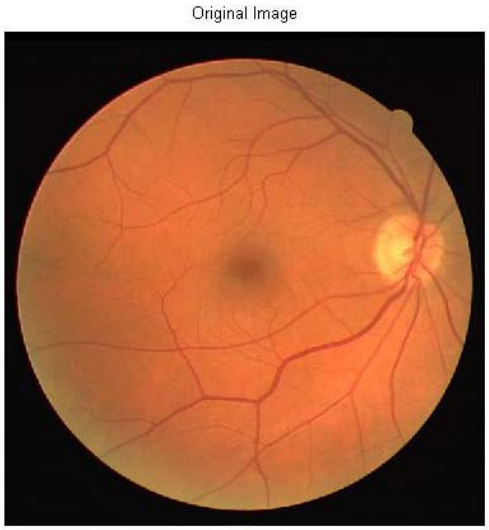

Figure 11 Original images from DRIVE dataset

The algorithm has been implemented by using Matlab version 7.9 (Release 2009 b) and is found to be reasonably fast and accurate than the existing computationally intensive methods. The results are promising even when it is applied to segment the vasculature in images with varying lighting or exposure levels and with varying pathologies like macular edema.

The proposed algorithm is simple and more efficient for automation. There is no mathematical complexity as in other methods and hence there is a significant improvement in computational time also. Moreover, this method does not just detect the vasculature but can extract the vascular tree also. The algorithm has been evaluated on a subset of the MESSIDOR and DRIVE image databases with various visual qualities. The corresponding ROC curve for the DRIVE dataset is shown in Fig. 9. It is found to be superior to the existing ones in terms of computational speed and accuracy. Several images with both eyes and with or without pathologies were also tested using the algorithm. The false alarm rate is found to be very less even in low contrast images with multiple defects.

Figure 12 Vasculature extracted by the algorithm

Figure 13 Ground truths (Gold standard) by the Human expert

Moreover, this method does not just detect the vasculature but can extract the pixels corresponding to vascular tree also. The algorithm, when implemented in matlab and executed on a Core i3 system with 4 GB memory took only 14 seconds for the segmentation, which is superior to the existing ones reported in the literature. The algorithm has been extensively tested on images of the MESSIDOR and DRIVE image databases with varying lighting and exposure levels and with varying levels of pathologies. It is found to be superior to the existing ones in terms of computational speed and accuracy. Several images of both eyes and with large areas of hemorrhages, microaneurysms and cotton wool spots were also

tested using the algorithm. The false alarm rate is found to be very low even in low contrast images with multiple defects. Our algorithm has a very promising average accuracy as depicted in Fig. 9. The main attraction of the proposed method is its simplicity, accuracy and saving in computational load. Moreover, unlike most other algorithms in this area, this algorithm does not require a prior knowledge of other retinal features such as optic disc or macula for the detection of vasculature .The method works pretty well to detect the narrow vessels even when the input image is a low-contrast one. The experimental results demonstrate that the proposed algorithm is fast, accurate and robust.

Conclusion

A novel algorithm for the extraction of vascular tree is proposed in this paper. The algorithm is superior to the existing algorithms in terms of computational time and accuracy.

Acknowledgement

The authors are highly indebted to MESSIDOR-TECHNO-VISION Project and the Image Sciences Institute's DRIVE database. The images were kindly provided by the program partners.

References

1. T. Ashok kumar, S. Priya and M.G. Mini. Fast optic disc localization and detection in retinal fundus images using bitplane decomposition and mathematical morphology, ***CIIT Int. Journal of Digital Image Processing***. 2011, 3: 431-448
2. T. Chanwimaluang, Guoliang Fan. An Efficient Blood Vessel Detection for Retinal Images Using Local Entropy Thresholding. ***Proc of ISCAS***. 2003, 5: 21-24
3. M.Sofka, C.V. Stewart. Retinal Vessel Extraction Using Multiscale Matched Filters, Confidence and Edge Measures. ***Technical Report***. 2005, 1-40,
4. S. Chaudhuri, S. Chatterjee, N. Katz, M. Nelson, and M. Goldbaum. Detection of Blood vessels in retinal images using two-dimensional Matched Filters. ***IEEE Trans Med Imag***. 1989, 8:263-269
5. A. Hoover, V. Kouznetsova, and M. Goldbaum. Locating blood vessels in retinal images by piecewise threshold probing of a matched filter response. ***IEEE Trans Med Imag.*** 2000, 19: 203-210
6. G. B. Kande, T. S. Savithri, and P. V. Subbaiah. Extraction of exudates and blood vessels in digital fundus images. ***Proceedings of 2008 IEEE 8th International Conference on Computer and Information Technology***. 2008, 526-513
7. J.J. Staal, M.D. Abramoff, M. Niemeijer, M.A. Viergever, B. Van Ginneken. Ridge based vessel segmentation in color images of the retina. ***IEEE Transactions on Medical Imaging***. 2004, 23:501-509
8. M. Akram, A. Tariq, and S. Khan. Retinal image blood vessel segmentation. ***International Conference on Information and Communication Technologies.*** 2009, 181-192
9. F. Oloumi, R. Rangayyan, P. Eshghzadeh-Zanjani, and F. Ayres. Detection of blood vessels in fundus images of the retina using Gabor wavelets. ***29th Annual Int. Conf. of the IEEE Engineering in Medicine and Biology Society.*** 2007, 6451-6454
10. C.Synthonyathin, J. F. Boyce, H. L. Cook, and T. H. Williamson. Automatic localisation of the optic disk, fovea, and retinal blood vessels from digital colour fundus images. ***Br J Ophthalmology***. 1999, 83:902-910
11. C. Sinthanayothin, J. F. Boyce, T. H. Williamson, H. L. Cook, E. Mensah, S. Lal, and D. Usher. Automated detection of diabetic retinopathy on digital fundus images. ***Diabet Med.*** 2002, 83:902-910
12. http://en.wikipedia.org/wiki/Adaptive_histogram_equalization.
13. http://en.wikipedia.org/wiki/Mathematical_morphology.
14. J.Serra, Image analysis and mathematical morphology, vol. 2, Academic Press, New York, 1988

15. G.D.Joshi, J.Sivaswamy. Colour Retinal Image Enhancement based on Domain Knowledge. ***6th Indian Conf. on Computer Vision, Graphics and Image Processing***. 2008, 591-598
16. http://www.who.int/mediacentre/factsheets/fs312/en/index.html. WHO fact sheet, November 2011
17. T. Ashok kumar, S. Priya and Varghese Paul. Automatic Feature Detection in Human Retinal Imagery Using Bitplane Slicing and Mathematical Morphology. ***European J of Sc Research***. 2012, *80:*57-67
18. http://messidor.crihan.fr, MESSIDOR Database.
19. http://www.isi.uu.nl/Research/Databases/DRIVE/, DRIVE Database.
20. D. Onkaew, R .Turior, Uyyanonvara B, Akinori N and C. Sinthanayothin. Automatic Vessel Extraction with combined Bottom-hat and Matched-filter**.** ***Int Conf on ICT for Embedded Systems***, Pattaya, Thailand. 2011, 101-105
21. T. Ashok kumar, S. Priya and Varghese Paul. A Novel Approach to the Detection of Macula in Human Retinal Imagery. ***Proc of IEEE Conf on ICECT****, 2012, 453-458*